Effect of Non-Linear Thermal Radiation and Partial Slip on Unsteady MHD Flow of a Nanofluid Past a Permeable Stretching Sheet through a Porous Medium with Suction/Injection Constant Heat and Mass Flix

Dr. Y. Madhusudhana Reddy
Associate Professor,
Dept of Mathematics,
Sri Venkateswara Degree & PG College,
Anantapur, Andhrapradesh-515001

Article Info
Page Number: 838 – 859
Publication Issue:
Vol 70 No. 1 (2021)

Abstract

This study deals with the effect of non-linear thermal radiation on the boundary layer flow of a thermophoretic magnetohydrodynamic dissipative nanofluid over an unsteady stretching sheet in a porous medium with temperature dependent internal heat source/sink with constant heat and mass flux. The governing equations are transformed to ordinary differential equations by using similarity transformation. Numerical solutions of these equations are obtained by using the Shooting Technique. The effects of non-dimensional governing parameters on the velocity, temperature, concentration profiles, friction factor, Nusselt and Sherwood numbers are discussed and presented through graphs and tables. Accuracy of the results compared with the existing ones. Excellent agreement is found with earlier studies.

Article Received:*12 November 2020*
Revised: *23 January 2021*
Accepted: *20 February 2021*
Publication*: 31 March 2021*

Keywords: - Non-linear thermal radiation, MHD, Thermophoresis, Dissipation, Stretching surface, Convection, constant heat and Mass flux.

1. Introduction

The development of nanotechnology is likely to bring unimaginable and multi-dimensional changes in our way of life, in the coming years. Recently many researchers focused on this topic due to its prominent importance in engineering and allied areas. Heat and mass transfer of thermophoretic magnetohydrodynamic flow has potential applications like air cleaning, aerosol particles sampling, nuclear reactor safety, micro electronics manufacturing etc. The detailed analysis on thermophoretic flows was discussed by Derjaguin and Yalamov [5]. The boundary layer flow of thermophoresis of aerosol particles over vertical flat plate was analyzed by Goren [10]. The term "nanofluid" was first introduced by Choi [4], Tsai [25]. Chamka and Issa [3]. He has given clear description about the heat transfer characteristics of nanofluids through MHD thermophoretic.

A similarity analysis for boundary layer flow by applying transverse magneticfield was studied by Ece [7]. Chemical reaction and radiation effects on Hiemenz flow in porous medium were studied by Seddeek et al. [23]. Radiation effect on mixed convection flow of micro polar fluid was discussed by Ibrahim et al. [11]. Philip et al. [17] discussed

thermophysical properties and heat transfer characteristics of nanofluids. Several authors (Afify [1], Bachok et al. [2], Seth et al. [24], Prasad et al. [18], Kabir and Mahbub [13]. Sandeep et al. [20]) proposed a similarity solution by considering suction/injection over stretching surface.

Thermophoretic MHD flow over isothermal vertical plate was studied by Noor et al. [16]. Yasin et al. [27] discussed the volume fraction effects on three types of nanofluids namely Cu-water, Al_2O_3-water and TiO_2 and they concluded that the type of nanofluid is important to increase the heat transfer rate. MHD on radiation effect on ethylene glycol based nanofluid over infinite vertical plate and porous medium have studied by Sandeep et al. [21 & 22]. MHD flow over stretching sheet with slip effects was discussed by Rushi Kumar [19], Manjulatha et al.[14], Mohan Krishna et al. [15], Uddin et al. [26], Dessie and Kishan [6], Ghalambaz and Noghrehabadi [9]

To the authors' knowledge no studies have been reported on the boundary layer flow of a thermophoretic MHD convective dissipative nanofluid over an unsteady stretching sheet in a porous medium by considering space and time dependent internal heat source/sink (non-uniform heat source/sink). In this study the governing equations are transformed to ordinary differential equations by using similarity transformation. Numerical solutions of these equations are obtained by using the Shooting Technique. The effects of non-dimensional governing parameters on the velocity, temperature, concentration profiles, friction factor, Nusselt and Sherwood numbers are discussed and presented through graphs and tables. Accuracy of the results to the existing ones and are found to be in excellent agreement with earlier studies.

2. Analysis Of The Flow

Consider an unsteady, incompressible, electrically conducting, two dimensional boundary layer flow of a dissipative nanofluid past a stretching sheet with non-uniform velocity $U_w(x, t)$ and permeability k'. The x-axis is along the continuous stretching surface and y axis is normal to the surface. An external magnetic field $B(x)$ is applied along the y direction. A non-uniform heat source/sink q''', suction/injection, thermophoresis effect along with volume fraction of nano

particles is taken in to account. No slip occurs between suspended particles and base fluid. The boundary layer equations that govern the present flow subject to the Boussinesq approximations can be expressed as

$$\frac{\partial u}{\partial x}+\frac{\partial v}{\partial y}=0 \tag{1}$$

$$\frac{\partial u}{\partial t}+u\frac{\partial u}{\partial x}+v\frac{\partial u}{\partial y}=\nu\frac{\partial^2 u}{\partial y^2}-\frac{\sigma \mathbf{B}_o^2}{\rho}u-(\frac{\nu}{k'})u+(1-C_\infty)(\rho_{f_\infty}\beta)g(T-T_\infty)- \\ -(\rho_p-\rho_{f\infty})\beta g(C-C_\infty) \tag{2}$$

$$\frac{\partial T}{\partial t}+u\frac{\partial T}{\partial x}+v\frac{\partial T}{\partial y}=(\frac{k_{nf}}{(\rho C_p)_{nf}})\frac{\partial^2 T}{\partial y^2}-\frac{1}{(\rho C_p)_{nf}}\frac{\partial q_R}{\partial y}+$$

$$+\tau(D_B\frac{\partial T}{\partial y}\frac{\partial C}{\partial y}\frac{D_T}{T_\infty}(\frac{\partial T}{\partial y})^2)+q'''+\frac{\nu}{C_p}(\frac{\partial u}{\partial y})^2$$

$$\frac{\partial C}{\partial t}+u\frac{\partial C}{\partial x}+v\frac{\partial C}{\partial y}=(D_B)\frac{\partial^2 C}{\partial y^2}+\frac{D_T}{T_\infty}(\frac{\partial^2 T}{\partial y^2}))-k_c(C-C_\infty)=0 \qquad (4)$$

The boundary conditions are

$$u=U_w(x,t)+A_{11}^{'}\frac{\partial u}{\partial y},v=v_w(x,t),-k_f\frac{\partial T}{\partial y}=q_w,-D_B\frac{\partial T}{\partial y}=m_w at\ y=0 \qquad (5)$$

$$u\to 0,T\to T_\infty,C\to C_\infty \qquad as\ y\to\infty$$

In equation(5) prime denotes differentiation with respect to y,where u and v are the velocity components in the x and y directions respectively.T,C are the temperature,concentration in the fluid,v_w is the suction /injection velocity with $v_w<0$ for suction, $v_{w>0}$ for injection, $\tau=\frac{(\rho C_p)_p}{(\rho C_p)_f}$, where $(\rho C_p)_p$ is the effective heat capacity of the nanoparticles, $(\rho C_p)_f$ is the heat capacity of the base fluid, $\frac{k_{nf}}{(\rho C_p)_{nf}}$ is the thermal diffusivity of the fluid, ν is the kinematic viscosity,D_B is the Brownian diffusion coefficient,D_T is the thermophoretic diffusion coefficient ,ρ i9s the fluid density,σ is the electrical conductivity, $B=B_o/\sqrt{1-ct}$ is the magnetic induction, $\dot{k}=k_0(1-ct)$ k is non-uniform permeability of the porous medium,kc is chemical reaction parameter q''' is the non-uniform heat source/sink,and λ is the stretching/shrinking parameter with $\lambda>0$ for stretching sheet and $\lambda<0$ for shrinking sheet.

Where $U_w(x,t)=\frac{ax}{1-ct}$ is the stretching sheet velocity, $V_w(x,t)=\frac{v_0}{\sqrt{1-ct}}$ is the mass transfer velocity,a is the initial stretching rate,c is the positive constant which measures the unsteadiness,We have a/(1-ct) is the initial stretching rate that increases with time.

The coefficient q''' is the rate of internal heat generation (>0) or absorption (<0). The internal heat generation /absorption q''' is modelled as

$$q'''=(\frac{k_f U_\infty(x,t)}{x\nu})(A_1(T_w-T_\infty)f'+B_1(T-T_\delta)) \qquad (6)$$

where $A_1^{'}$ and $B_1^{'}$ are coefficients of space dependent and temperature dependent internal heat generation or absorption respectively. It is noted that the case $A_1^{'}>0$ and $B_1^{'}>0$, corresponds to internal heat generation and that $A_1^{'}<0$ and $B_1^{'}<0$, the case corresponds to internal heat absorption case.

Using Roseland approximation the radiative heat flux q_r is given by

$$q_r=\frac{-4\sigma^*}{\beta_R}\frac{\partial}{\partial y}(T^{1^4}) \qquad (7)$$

and expanding T^{1^4} about T_∞ by Taylor's expansion

$$T^{1^4} = 4T_\infty^3 T^1 - 3T_\infty^4 \tag{8}$$

Using (6) & (7) equation (3) reduces to

$$\left.\begin{aligned}\frac{\partial T}{\partial t} + u\frac{\partial T}{\partial x} + v\frac{\partial T}{\partial y} = \left(\frac{k_{nf}}{(\rho C_p)_{nf}}\right)\frac{\partial^2 T}{\partial y^2} - \frac{1}{(\rho C_p)_{nf}}\left(\frac{16\sigma^{\div}\beta_R T_\infty^3}{3\beta_R}\right)\frac{\partial^2 T}{\partial y^2} + \\ + \tau\left(D_B\frac{\partial T}{\partial y}\frac{\partial C}{\partial y}\frac{D_T}{T_\infty}\left(\frac{\partial T}{\partial y}\right)^2\right) + \frac{\nu}{C_p}\left(\frac{\partial u}{\partial y}\right)^2 + \left(\frac{k_f U_\infty(x,t)}{x\nu}\right)(A_1(T_w - T_\infty)f' + B_1(T - T_\delta))\end{aligned}\right| \tag{9}$$

The non-dimensional temperature $\theta(\eta) = \frac{T - T_\infty}{T_w - T_\infty}$ can be simplified as

$$T = T_\infty(1 + (\theta_w - 1)\theta) \tag{10}$$

Where $\theta = \frac{T_w}{T_\infty}$ is the temperature parameter

Introducing the similarity variables as

$$\left.\begin{aligned}\psi = \left(\sqrt{a\nu/(1-ct)}\right)xf(\eta),,\eta = y\sqrt{\frac{a}{\nu(1-ct)}}\ ,\theta(\eta) = \frac{T - T_\infty}{(q_w/k_f)},\phi(\eta) = \frac{c - c_\infty}{(m_w/D_B)} \\ T = T_w(x,t) = T_\infty + \frac{ax}{1-ct}\theta(\eta), C = C_w(x,t) = C_\infty + \frac{ax}{1-ct}\phi(\eta)\end{aligned}\right. \tag{11}$$

Where the stream function ψ is defined as $u = \frac{\partial\psi}{\partial y}, v = -\frac{\partial\psi}{\partial x}$ which automatically satisfies the continuity equation(1)..Further $\theta(\eta)$, $f(\eta)$ and $\phi(\eta)$ are dimensionless stream function,temperature and concentratrion functions respectively.

$$u = \frac{ax}{1-ct}f'(\eta), v = -\sqrt{\frac{a\nu}{1-ct}}f(\eta) \tag{12}$$

Substituting (11) in equations (2,3, and 9) we get

$$f''' + ff'' - (f')^2 - \frac{S}{2}\eta f'' - (S + M^2 + D^{-1})f' + G(\theta - N\phi) = 0 \tag{13}$$

$$\left.\begin{aligned}Rd((1 + (\theta_w - 1)\theta)^3)\theta')' - S(\theta + \frac{1}{2}\eta\theta') + Nb\theta'\phi' + Nt(\theta')^3 + A_1 f' + B_1\theta + \\ + \ \Pr(f\theta' - f'\theta) + Ec(f')^2 = 0\end{aligned}\right| \tag{14}$$

$$\phi'' + \left(\frac{Nt}{Nb}\right)\theta'' + Le(f\phi' - f'\phi - \gamma\phi) - LeS(\phi + \frac{1}{2}\eta\phi') = 0 \tag{15}$$

Where prime denote differentiation with respect to η .

The transformed boundary conditions are

$$\left.\begin{aligned}f(0) = f_w,\ f'(0) = 1 + A_{11}f''(0), \theta'(0) = -1, \phi'(0) = -1 \\ f'(\eta) \to 0, \theta(\eta) \to 0, \phi(\eta) \to 0 \qquad as\ \eta \to \infty\end{aligned}\right. \tag{16}$$

Where S=c/a is the unsteady parameter

$\Pr = \frac{\mu C_p}{k_f}$, (Prandtl number), $Le = \frac{\nu}{D_B}$, (Lewis number), $Nb = \frac{\tau D_B (C_w - C_\infty)}{\nu}$ (Brownian motion parameter), $Nt = \frac{\tau D_T (T_w - T_\infty)}{\nu T_\infty}$ (Thermophoresis parameter), $Rd = \frac{4\sigma^{\bullet} T_\infty^3}{\beta_R k_f}$, (Thermal radiation parameter), $M^2 = \frac{\sigma B_0^2}{a\rho_f}$, (Magnetic parameter), $Q = \frac{Q_H \nu}{(\rho_{f\infty} C_p)_f c k_f}$ (Heat source parameter), $f_w = \frac{v_o}{\sqrt{\nu x}}$ (suction parameter), $Ec = \frac{U_w^2}{C_p (T_w - T_\infty)}$ (Eckert number), $D^{-1} = \frac{\nu}{ak'}$ (Inverse porous parameter), $\gamma = \frac{k_c C_\infty \nu}{D_B}$, (Chemical reaction parameter), $A_{11} = A_{11}' \sqrt{\frac{a}{\nu}} (> 0)$ (first order slip parameter), $A = \theta_w$ (temperature ratio)

3.Numerical Method For Solutions:

The above equations (13)-(15) aliong with the boundary conditions are solved by converting them to an initial value problem.We set

$f_1 = f, f_2 = f', f_3 = f_2' = f'',]$

$$f_4 = f''' = -f_1 f_3 + (f_2)^2 + \frac{S}{2}\eta f_3 + (S + M^2 + D^{-1}) f_2 - G(f_5 - N f_7) \qquad (17)$$

$$f_5 = \theta, f_6 = \theta', f_7 = \theta'' = -[Nb f_6 f_9 + Nt(f_6)^3 - (A_1 f_2 + B_1 f_5) + \\ + \Pr(f_2 f_5 - f_1 f_6) - 3Rd(A-1)^3 (f_5 f_6)^2 - 6Rd(A-1)^2 f_5 f_6^2 - 3Rd(A-1) f_6^2) + \qquad (18) \\ + S(f_5 + 0.5\eta f_{6)}]/[1 + Rd(A-1)^3 f_5^3 + 3Rd(A-1)^2 f_5^2 + 3Rd(A-1) f_5]$$

$$f_8 = \phi, f_9 = \phi', f_{10} = \phi'' = -[(\frac{Nt}{Nb}) f_7 + Le(f_1 f_9 - f_2 f_8 - \gamma f_8 + S(f_8 + 0.5\eta f_9))] \qquad (19)$$

with the boundary conditions

$$f_1(0) = f_w, f_2(0) = 1 + A_{11} f_3(0), f_6(0) = -1, f_9(0) = -1$$

$$f_2(\eta) \to 0, f_5(\eta) \to 0, f_8(\eta) \to 0 \qquad as \ \eta \to \infty \qquad (20)$$

In order to integrate (14) –(16) as an initial value problem one requires a value for $f_3(0)$,that is $f''(0)$, $f_6(0)$,that is $\theta'(0)$, $f_9(0)$,that is $\phi'(0)$ but no such values are give3n at the boundary.The suitable guess values for $f''(0), \theta'(0)$ and $\phi'(0)$ are chosen and the n integration is carried out.Comparing the calculated values for f'', θ' and ϕ' at η=10(say) with the given boundary conditions $f'(10) = 0, \theta(10) = 0$ and $\phi(10) = 0$ and adjusting the estimated values , $f''(0), \theta'(0)$ and $\phi'(0)$,we apply the fourth order classical Runge-Kutta method with step size h=0.01.The above procedure is reported un til we get the converged result within a tolerance limit of 10^{-5}.

The coefficient of skin friction coefficient C_{fx} and reduced Nusselt number Nux and reduiced Sherwood number Shx are given by

$$C_{fx} = \frac{x\mu}{\rho u_w^2}(\frac{\partial u}{\partial y})_{y=0}, Nux = \frac{x}{(T_w - T_\infty)}(\frac{q_w}{k_f})_{y=0}, Shx = \frac{x}{(C_\infty)}(\frac{\partial C}{\partial y})_{y=0},$$

using (9) and (13),we get

$$R_{ex}^{1/2} C_{fx} = f''(0)\ ,\ R_{ex}^{-1/2} Nux = 1/\theta(0)\ ,\ R_{ex}^{-1/2} Shx = 1/\phi(0)$$

where $R_{ex} = \frac{xu_w}{\nu}$ is the local Reynolds number.

Method of Solution:

The coupled non-linear equations(10)-(12) with associated boundary conditions(13) are solved numerically using shooting iteration method together with fourth order Runge-Kutta method .The initial conditions for $f''(0)$, $\dot{\theta}(0)$ and $\phi'(0)$ are presumed and then integrated numerically as an initial value problem.The symbolic software MATHEMATICA is used for computational work.To obtain the numerical solutions the maximum value of η is taken as 6.This process is continued until the results achieve the designed degree of accuracy ,namely 10^{-7} .

4. Comparision:

Table.1 : Comparison of $-\theta'(0)$ values when Nb=Nt=Ec=A1=B1=K=M=G=N=A1=0

A	ξ	Pr	Ishak et al [12]	Ferdowsi et al [8]	**Present study**
0	0.5	0.71	0.4370	0.4564	**0.4558**
0	0.5	1	0.5000	0.5000	**0.5002**
0	0.5	10	0.6452	0.6450	**0.6455**
0	1	0.61	0.0197	0.0191	**0.01094**
0	1	0.72	0.8086	0.8082	**0.8089**
0	1	1	1.0000	1.0000	**1.0002**
0	1	3	1.9237	1.9229	**1.9233**
0		10	13.7207	3.7201	**3.7205**
0	2	0.71	1.4944	1.4944	**1.4944**
0	2	1	2.0000	2.0000	**2.0002**
0	2	10	16.0842	16.0835	**16.0833**
1	0.5	1	0.8095	0.8086	**0.8087**
1	1	1	1.3201	1.3201	**1.3202**
1	2	1	2.2219	2.2219	**2.2221**

5. Results And Discussion

The system of nonlinear ordinary differential equations (11) to (13) with the boundary conditions (14) are solved numerically using Fourth order Runge-Kutta Shooting technique with MATHEMATICA package. The results obtained shows the influences of the non dimensional governing parameters, namely thermal radiation parameter *Rd*, chemical reaction parameter γ, magnetic field parameter *M* , Brownian motion parameter *Nb* , viscous dissipation parameter *Ec* and thermophoresis parameter *Nt* on velocity, temperature,

nanoconcentration, skin friction and local Nusselt numbers are thoroughly investigated for stretching and shrinking cases separately and presented through graphs and tables. For numerical results we considered Pr=6.2,*Nb=Nt=0.3,D-1=0.2,Le=2, M=, N=0.5, γ=0.5, A11=0.2,* Ec=0.01, A=1.05 In entire study these values kept as common except the varied values as displayed in figures. From the variation of velocity, temperature and nanoconcentration with different parameters we find that the temperature is positive for all variations.

The variation of velocity, temperature and nanoconcentration with Grashof number G if exhibited in figs,2a-2c.From the profiles we find that higher the thermal buoyancy(G)larger the velocity and smaller the temperature in the flow region.This may be attrributed to the fact increase in G leads to a grow momentum boundary layer and decay in thermal boundary layer.From fig.2c we notice that the nanoconcentration enhances in the flow region with increase in G.

Figures 3a-3c depicts the effect of magnetic field parameter on velocity, temperature and nanoconcentration profiles for stretching case. It is evident from figures that increase in magnetic field parameter decreases the velocity and nanoconcentration profiles and increases the temperature .Generally increase in magnetic field generates the opposite force to the flow, called Lorentz force. The reason for increase in the temperature and nanoconcentration profiles in stretching case is the increase in magnetic field grows the thermal and decays the solutal boundary layer thicknesses.

Figs.4a-4c represent the effect of porous parameter(D^{-1}).on the velocity, temperature and nanoconcentration.Lesser the permeability of the porous medium smaller the velocity and nanoconcentration and larger the temperature..This may be due to the fact that an increase in D^{-1} reduces the momentum and solutal boundary layer thickness and grows the thermal boundary layer thickness with increase in D^{-1}.

The effect of buoyancy ratio(N) can be seen from figs.5a-5c.From the profiles we find that when the molecular buoyancy force dominates over the thermal buoyancy force the velocity, nanoconcentration reduces and the temperature enhances when the buoyancy forces are in the same direction.This is because an increase in N decays the thickness of the momentum,solutal boundary layers and grows the solutal boundary layer thickness.

Figures 6a-6c displays the effect of Brownian motion parameter (Nb) on velocity, temperature and nanoconcentration profiles.It is clear from figures that increase in Brownian motion parameter enhances the temperature and depreciates the velocity and nanoconcentration in the boundary layer.The reason behind this is different nano particles have different values of Brownian motion parameter which leads to enhance the heat transfer rate.

The effects of thermophoresis parameter(Nt) on velocity, temperature and nanoconcentration profiles for stretching and shrinking cases re presented in figures 7a-7c. It is observed that increases in thermophoresis parameter depreciates the velocity and develops temperature and nanoconcentration profiles of the flow (figs.7a-7c).This may be attributed to the fact increase in Nt leads to thickening of the thermal and solutal boundary layers and thinning of the momentum boundary layer.

Figs.8a-8c and 9a-9c depict the variation of velocity,temperature and nanoconcentration with space heat source parameter(A1) and temperature dependent h\eat source(B1).In the presence of space dependent / temperature dependent heat generating source(A1>0,B1>0) energy is generated in the boundary layer which results in an increment in velocity and temperature while in the case of heat absorbing source(A1<0)or (B1<0) they experience a reduction due to the absorption of energy in the boundary layer.The nanoconcentration reduces with A1>0 /B1>0 and enhances with A1<0/B1<0 in the entire flow region.

Figs.10a-10c represent the variation of velocity, temperature and nanoconcentration with unsteady parameter(S).From the profiles we find that the velocity enhances, temperature and nanoconcentration depreciate with increase in S.This may be attributed to the fact that an increase in unsteady parameter grows the thickness of the momentum, and decays the thermal and solutal boundary layers.

The effect of chemical reaction parameter(γ) on velocity, temperature and nanoconcentration profiles are illustrated in figs.11a-11c.The velocity enhances,temperature and nanoconcentration reduce in the degenerating chemical reaction case($\gamma>0$). while a reversed effect is noticed in their behaviour in generating case($\gamma<0$).This agrees the physical fact that chemical reaction parameter have tendency to reduce the nanoconcentration boundary layer thickness. We observed significant variation in temperature profiles due to increase in chemical reaction parameter. It may happen due to the fact that chemical reaction helps to reduce the mass transfer and decays the solutal boundary layer thickness.

Fiugs.12a-12c depict the variation of velocity, temperature and nanoconcentration with thermal radiation parameter(Rd).From the profiles we find that higher the radiative heat flux larger the velocity and temperature. The nanoconcentration reduces in the flow regions (0.4.0) with increasing Rd.

Figures.13a-13c illustrate the influence of viscous dissipation parameter(Ec) on velocity, temperature and nanoconcentration profiles. It is clear from figures that increase in viscous dissipation parameter enhances the velocity and temperature profiles over stretching surface.The nanoconcentration reduces in the flow region with higher values of Ec.This may be due to the fact that an increase in Ec results in growth of the momentum and thermal boundary layer thickness.The solutal boundary layer thickness decays with Ec.

Figs. 14a-14c show the influence of suction/injection parameter (fw) on velocity, temperature and nanoconcentration profiles.. It is clear that an increase in suction parameter (fw>0)depreciates the velocity, temperature and enhances the nanoconcentration in the boundary layer and with injection parameter(fw<0),a reversed behaviour id noticed in their behaviour.Thus the momentum and thermal boundary layers decay with fw>0 and grows with fw<0.

The effect of temperature ratio(A) on f',θ and ϕ can be seen from figs.15a-15c.From the profiles we find that an increase in temperature ratio(A) enhances the velocity, temperature and reduces the nanoconcentration.Thus the non-linearity in thermal radiation leads to a growth in momentum and thermal boundary layers thickness and decay in solutal boundary layer thickness.,.

The effect of first order slip(A11) on f′,θ and ϕ can be seen from figs.16a-16c.From the profiles we find that an increase in A11 reduces the velocity in a the region(0,1.0) and enhances in the flow region(1.0,4.0).The temperature increases and the nanoconcentration reduces with increasing values of A.This may be attributed to the fact that an increase in slip parameter leads to thinning of the momentum and solutal boundary layers while the thickness of the thermal boundary layer grows with A11.

From figs 17a-17c we find that an increase in Lewis number enhances the velocity and reduces the temperature, nanoconcentration in the boundary layer.An increase in Le amounts to reduction in Brownian diffusion co-efficient. For a fluid of certain kinematic viscosity υ a higher Lewis number corresponds to a lower diffusion co-efficient D_B which results in a smaller penetration depth for the nanoconcentration boundary layer.

Figs.18a-18c depict the influence of Prandtl number(Pr) on velocity ,temperature and nanoconcentration.From the profiles we find that lesser the thermal diffusivity smaller the velocity , temperature and larger the nanoconcentration .Thus the thermal boundary thickness reduces and solutal layer thickness grows with increasing values of Pr.

Table 2 shows the variation in skin friction coefficient, Nusselt and Sherwood numbers for different values of non dimensional governing parameters for stretching case. From the table at the given range of values we find an increase in G reduces the skin friction(τ) with $G\leq 4$ and for higher $G\geq 6$,it enhances on $\eta=0$.The rate of heat transfer enhances,mass transfer rate enhances on the wall with increase in G.An enhancement in the skin friction, mass transfer rate and a fall in heat transfer rate is noticed by increasing magnetic field parameter(M),.With respect to inverse darcy parameter(D-1), larger skin friction,,Sherwood number and Nusselt number at the wall. Higher the viscous dissipation parameter(Ec) larger the skin friction,Nu and smaller Sh on $\eta=0$.When the molecular buoyancy force dominates over the thermal buoyancy force, larger skin friction,Sh and smaller Nu on the wall when the buoyancy forces are in the same direction.An increase in space dependent/temperature dependent heat source parameters ($A1,B1>0$) decreases τ,Nu and enhances Sh on the wall while a reversed effect is notice inn them with $A1<0,B1<0$).An increase in Brownian motion parameter(Nb) reduces skin friction, and enhances Nusselt and Sherwood numbers on $\eta=0$.An increase in thermophoretic parameter(Nt) enhances skin friction,reduces the Nusselt and Sherwood numbers at the wall.Higher the radiative heat flux larger skin friction, Nusselt and Sherwood numbers on $\eta=0$.The skin fricftion reduces,Numer and Sherwood number enhance in both degenerating /generating chemical reaction cases.τ,Nu enhance with $fw>0$ and reduces with $fw<0$.The Sherwood number reduces with $fw>0$ and enhances with $fw<0$.An increase in unsteady parameter($S\leq 0.2$) reduces skin friction and for higher $S\geq 0.3$,we notice an increment in the skin friction.The Nusselt and Sherwood numbers on the wall enhance with increasing values of S.. An increase in first order slip parameter(A11) /temperature ratio(A) reduces skin friction,Nusselt number and enhances Sherwood number on the wall.Higher the Lewis number(Le) smaller the skin friction and larger Nu and Sh.Lesser the thermal diffusivity larger the skin friction,Nusselt number and smaller the Sherwood number on $\eta=0$.

6. Conclusions

This paper presents the effect of non-linear thermal radiation on two dimensional unsteady convective hydromagnetic heat transfer flow of a nanofluid past a permeable stretching sheet in a porous medium with suction/injection effects. The governing partial differential equations are reduced in to ordinary differential equations by similarity transformation and then solved numerically by using Runge-Kutta fourth order technique along with Shooting method.

The findings of the numerical results are summarized as follows:

1) Magneticfield parameter has capability to reduce the velocity, nanoconcentration and enhances the temperature..Skin friction,Sherwood number enhances,Nusselt number reduces on the wall with increasing M.
2) Radiation parameter helps to enhance the velocity,temperature profiles, skin friction,heat and mass transfer rates of the fluid and reduce the nanoconcentration profiles
3) Chemical reaction parameter enhances heat and mass transfer rates as well as velocity profiles.The temperature and nanoconcentration reduce with increasing γ.
4) Viscous dissipation parameter helps to enhance the velocity,temperature profiles reduces the nanoconcentration.Skin friction factor ,Nusselt number reduce,Sherwood number enhances with Ec.,
5) Suction parameter($fw>0$) have tendency to increase the friction factor,heat transfer rate and nanoconcentration and reduces with $fw<0$ on $\eta=0$.
6) Higher the unsteady parameter(S) larger the velocity,heat and mass transfer rates,smaller the temperature ,nanoconcentration.
7) An increase in slip parameter(A11).reduces the velocity,enhances the temperature and nanoconcentration .τ,Nu reduce and Sh increases with increasing A11 on $\eta=0$.
8) Higher Brownian motion parameter(Nb) larger velocity,Nu and Sh on the wall.It reduces the temperature , nanoconcentration and skin friction .
9) An increase in Nt enhances temperature, nanoconcentration,Skin friction .velocity,Nuseelt and Sherwood numbers experience reduction with increasing values of Nt.
10) An increase in buoyancy parameter(N) reduces the velocity,nanoconcentration and reduces temperature.Skin friction,Sherwood number increase and Nusselt number reduces with increase in N.
11) The non-linearity in thermal radiation($A=\theta w$)leads to an enhancement in velocity,temperature,Sherwood number and reduction in nanoconcentration,Skin friction and Nusselt number.

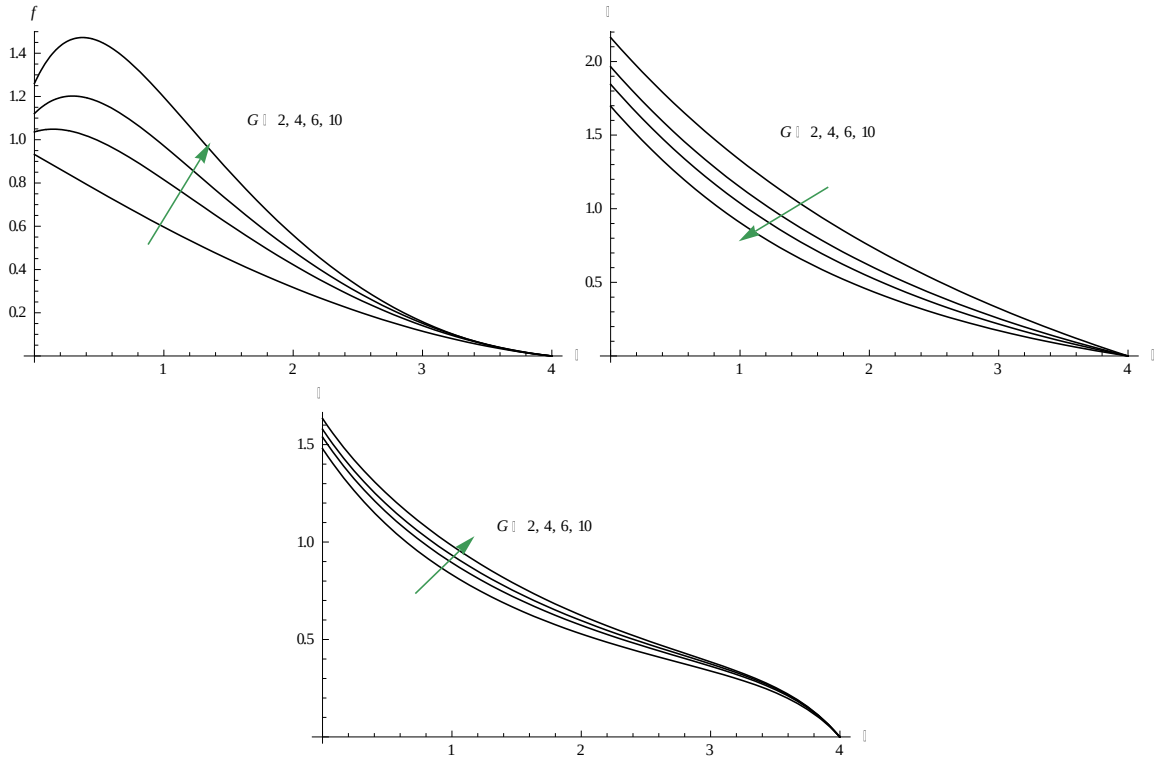

Fig.2 : [a] Variation of velocity(f'), [b] Temperature(θ), [c] Nano-Concentration(ϕ) with G
M=0.5N=0.5Rd=0.5Ec=0.01γ=0.5Nb=0.3Nt=0.3
A1=0.5B1=0.5S=0.1fw=0.2,A=1.05,A11=0.2Le=10Pr=0.71

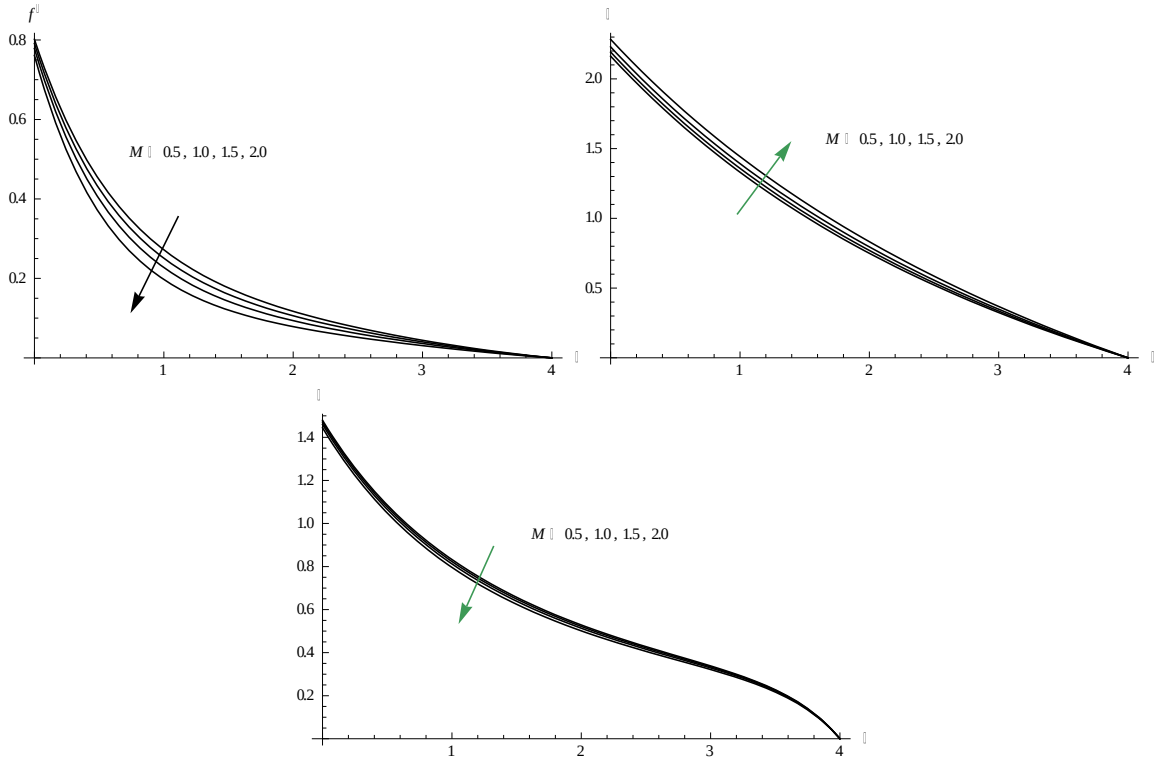

Fig.3 : [a] Variation of velocity(f'), [b] Temperature(θ), [c] Nano-Concentration(ϕ) with M
G=2N=0.5Rd=0.5Ec=0.01Nb=0.3Nt=0.3
A1=0.5S=0.1fw=0.2,A=1.05,A11=0.2Le=10Pr=0.71

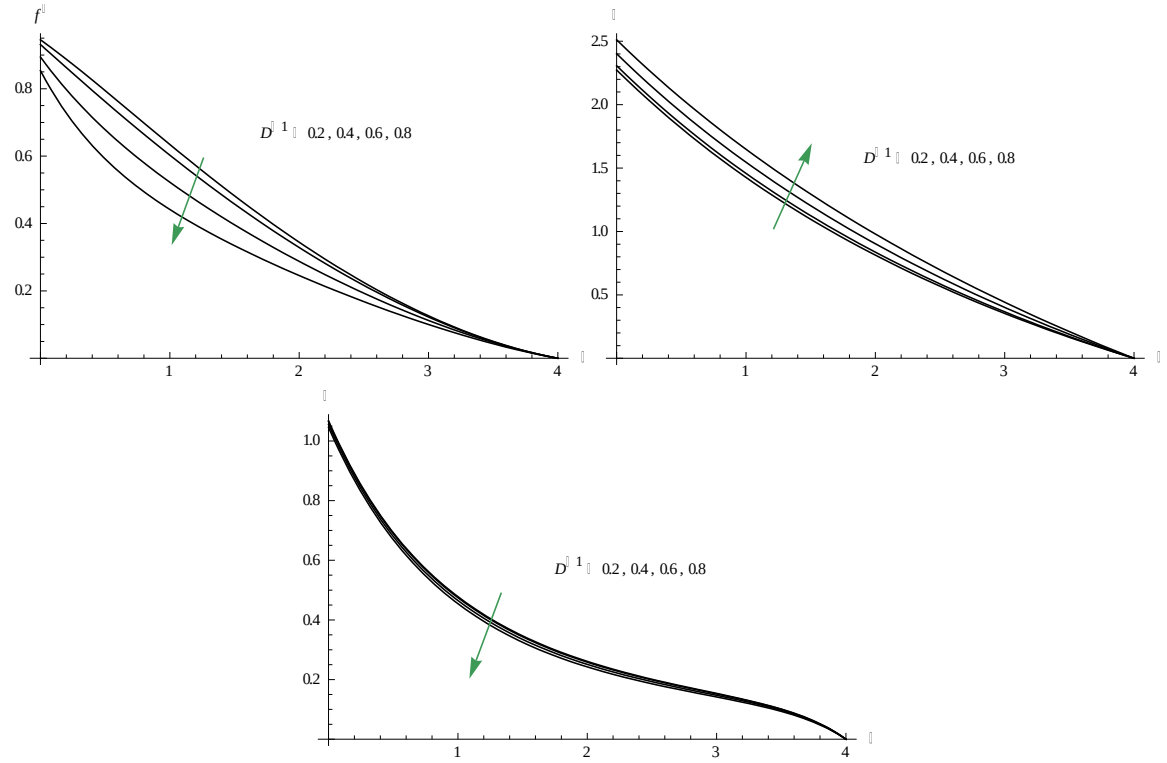

Fig.4 : [a] Variation of velocity(f'), [b] Temperature(θ), [c] Nano-Concentration(ϕ) with D^{-1}
M=0.5N=0.5Rd=0.5Ec=0.01γ=0.5Nb=0.3Nt=0.3
A1=0.5B1=0.5S=0.1fw=0.2,A=1.05,A11=0.2Le=10Pr=0.71

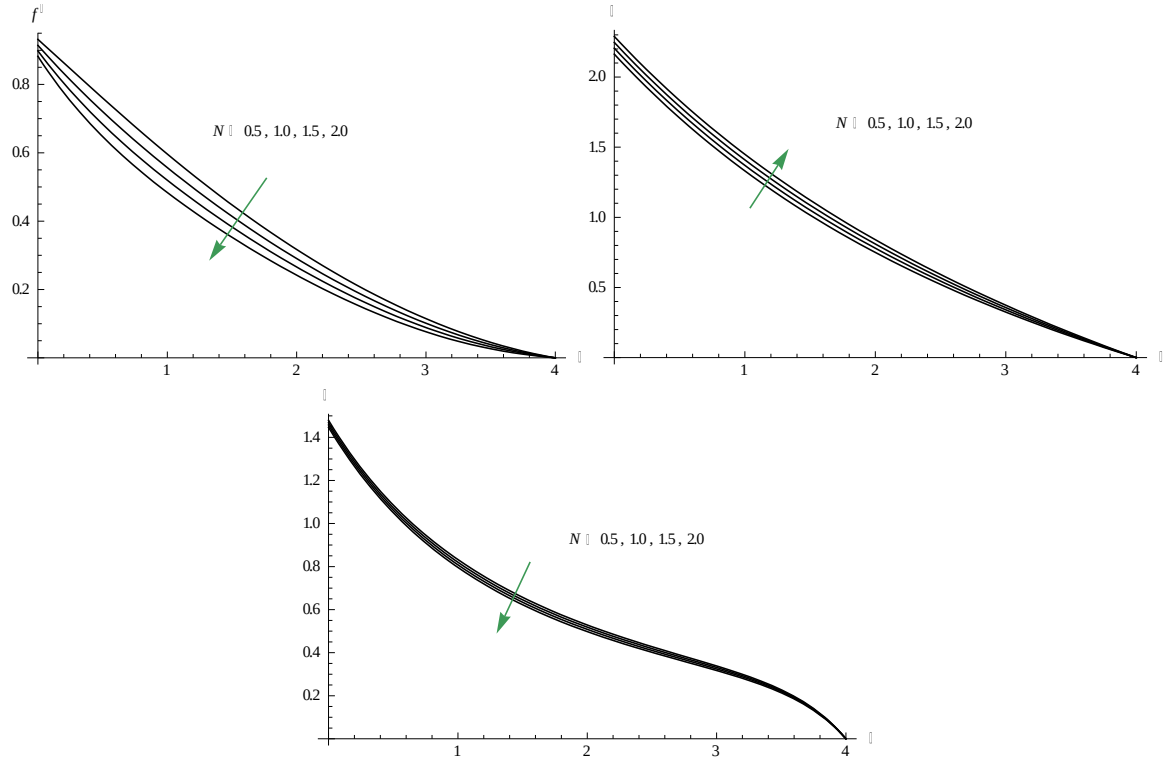

Fig.5 : [a] Variation of velocity(f'), [b] Temperature(θ), [c] Nano-Concentration(ϕ) with N
G=2M=0.5Rd=0.5Ec=0.01γ=0.5Nb=0.3Nt=0.3

A1=0.5B1=0.5S=0.1fw=0.2,A=1.05,A11=0.2Le=10Pr=0.71

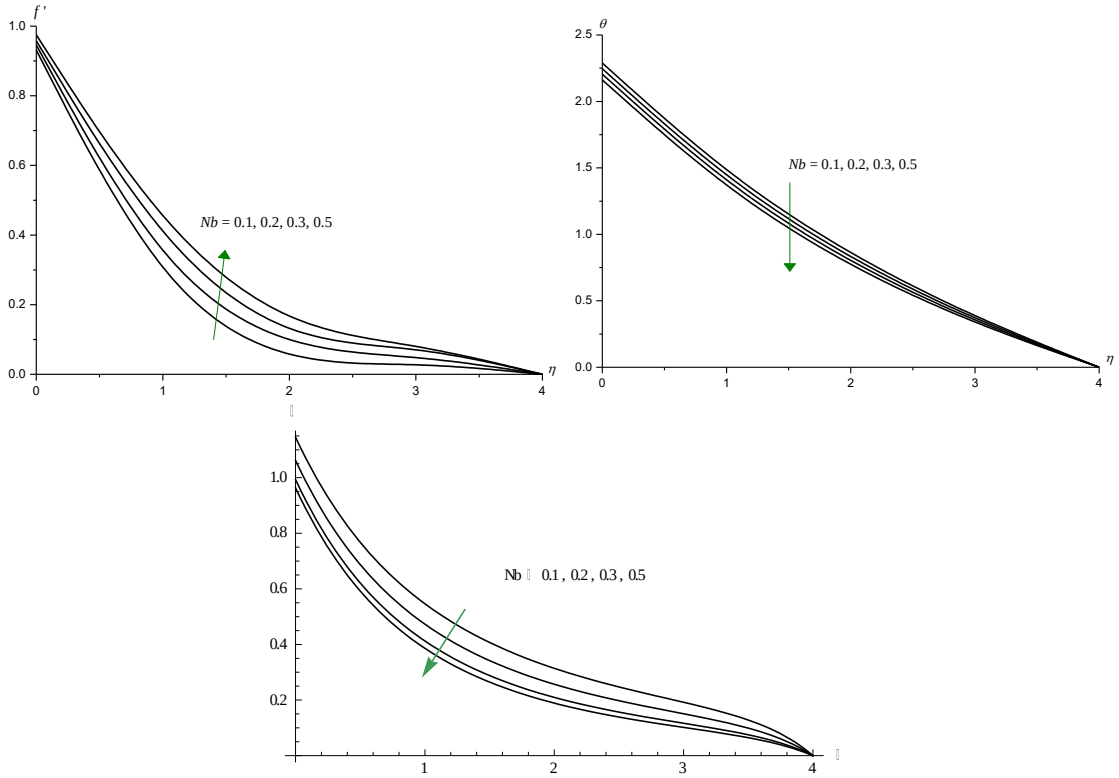

Fig.6 : [a] Variation of velocity(f'), [b] Temperature(θ), [c] Nano-Concentration(ϕ) with Nb

G=2M=0.5N=0.5Rd=0.5Ec=0.01γ=0.5Nt=0.3

A1=0.5B1=0.5S=0.1fw=0.2,A=1.05,A11=0.2Le=10Pr=0.72

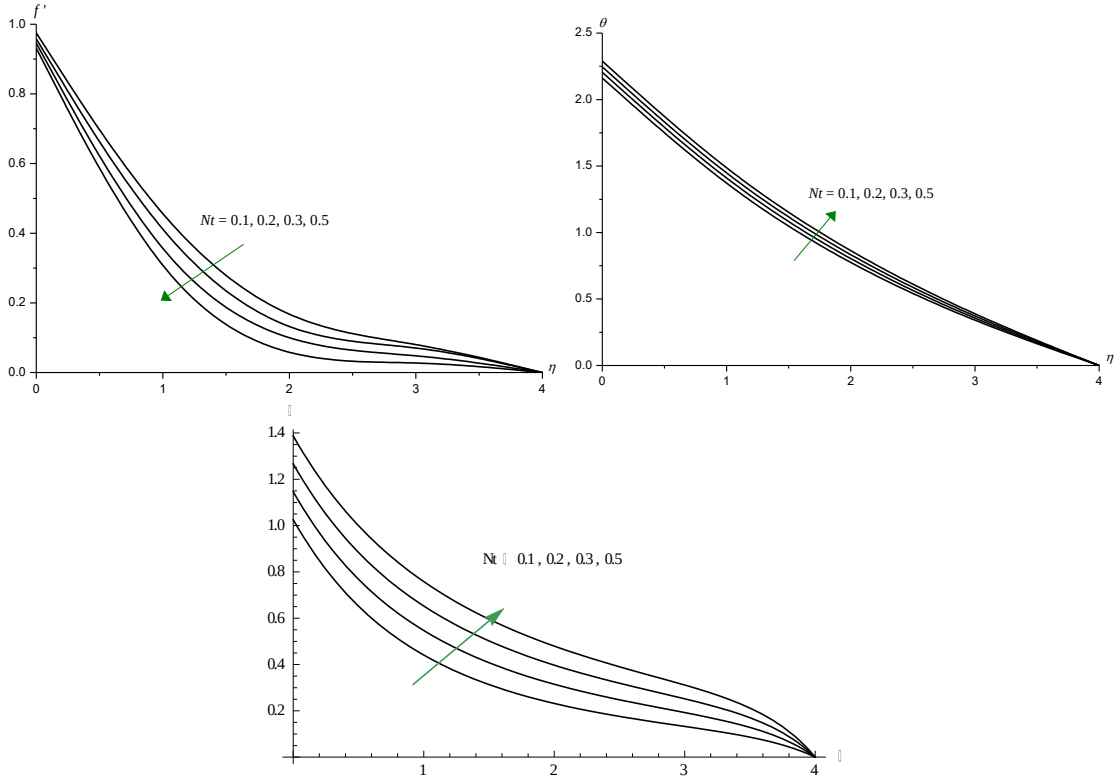

Fig.7 : [a] Variation of velocity(f'), [b] Temperature(θ), [c] Nano-Concentration(ϕ) with Nt

M=0.5N=0.5Rd=0.5Ec=0.01Nb=0.3
A1=0.5S=0.1fw=0.2,A=1.05,A=011.2Le=10Pr=0.71

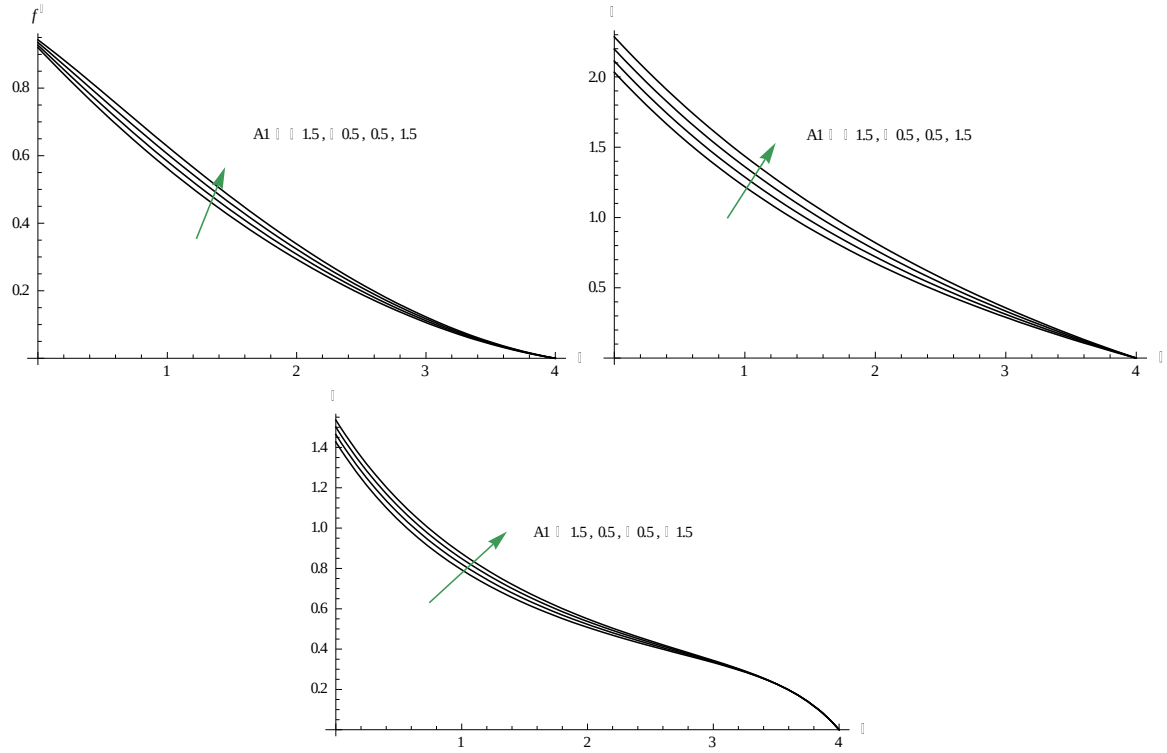

Fig.8 : [a] Variation of velocity(f'), [b] Temperature(θ), [c] Nano-Concentration(ϕ) with A1
G=2M=0.5N=0.5Rd=0.5Ec=0.01γ=0.5Nb=0.3
Nt=0.3B1=0.5S=0.1fw=0.2,A=1.05,A11=0.2Le=10Pr=0.71

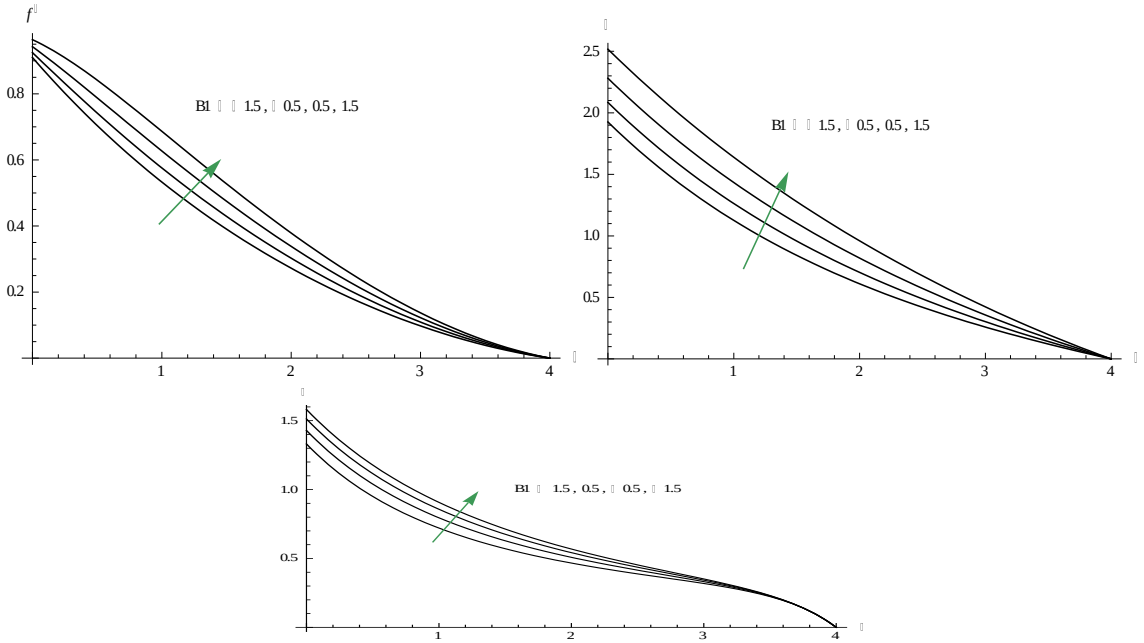

Fig.9 : [a] Variation of velocity(f'), [b] Temperature(θ), [c] Nano-Concentration(ϕ) with B1
M=0.5N=0.5Rd=0.5Ec=0.01Nb=0.3Nt=0.3
A1=0.5S=0.1fw=0.2.A=1.05,A11=0.2Le=10Pr=0.71

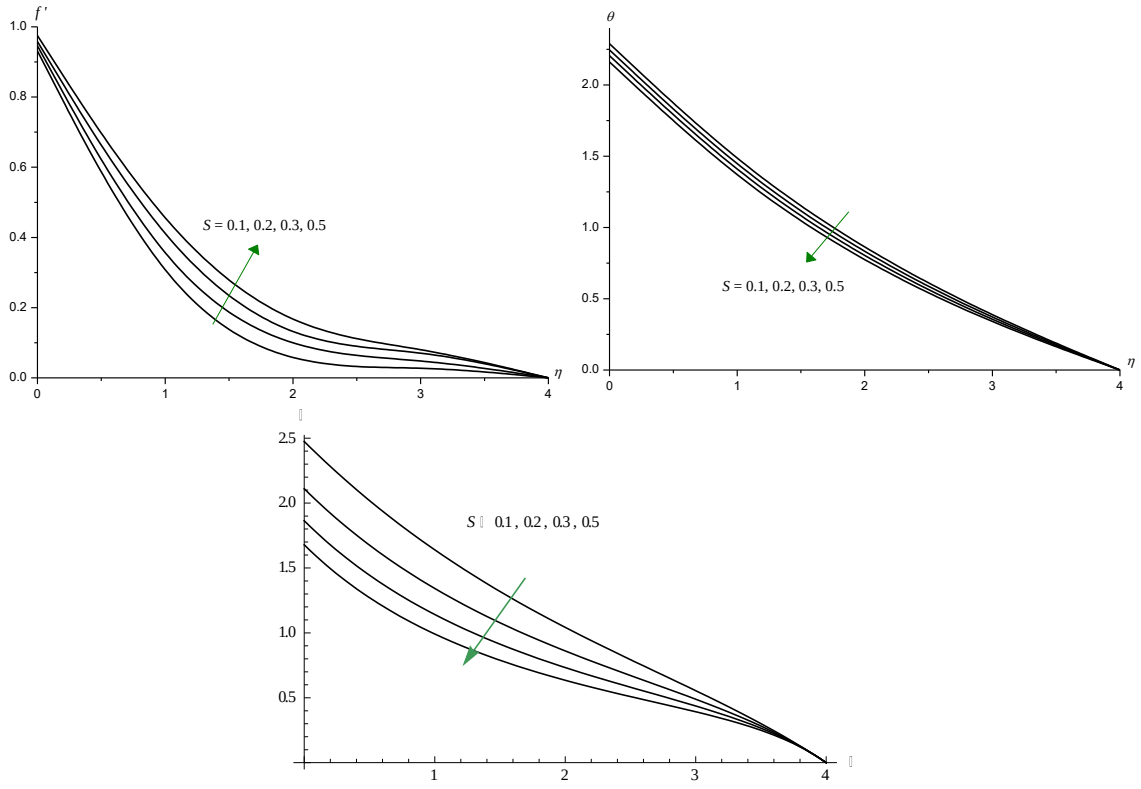

Fig.10 : [a] Variation of velocity(f'), [b] Temperature(θ), [c] Nano-Concentration(ϕ) with S
M=0.5N=0.5Rd=0.5Ec=0.01Nb=0.3
Nt=0.3G=2fw=0.2,A=1.05,A11=0.2Le=10Pr=0.71

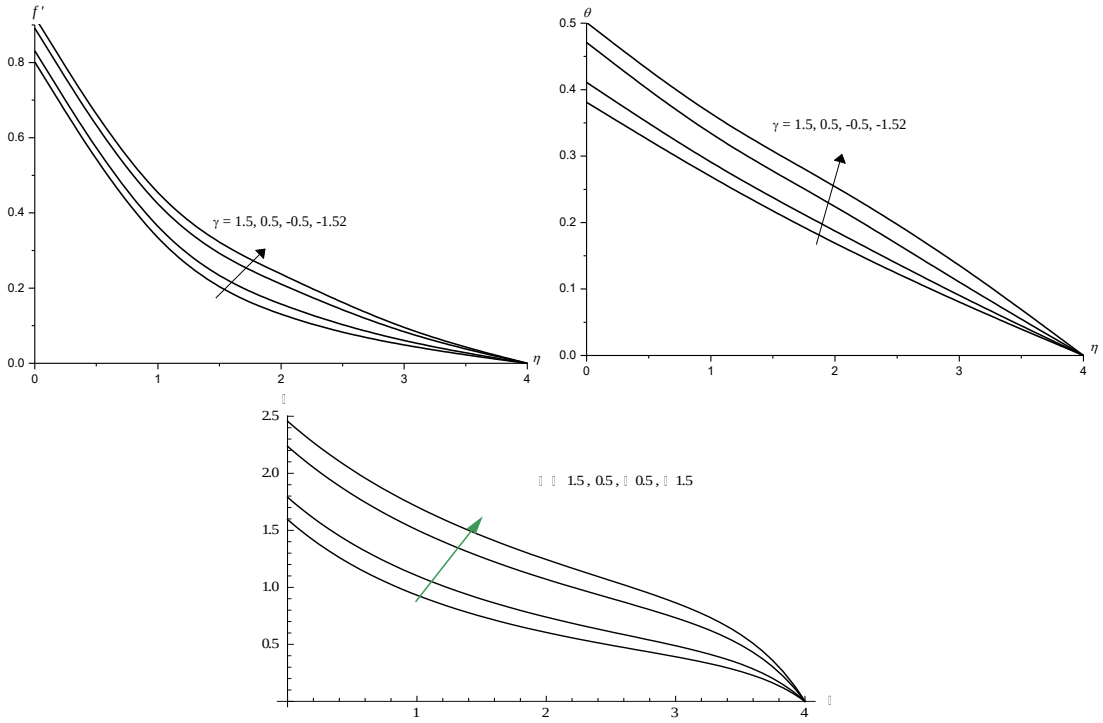

Fig.11 : [a] Variation of velocity(f'), [b] Temperature(θ), [c] Nano-Concentration(ϕ) with γ
M=0.5N=0.5Rd=0.5Ec=0.01Nb=0.3A1=0.5
B1=0.5Nt=0.3S=0.1fw=0.2.A=1.05,A11=0.2Le=10Pr=0.71

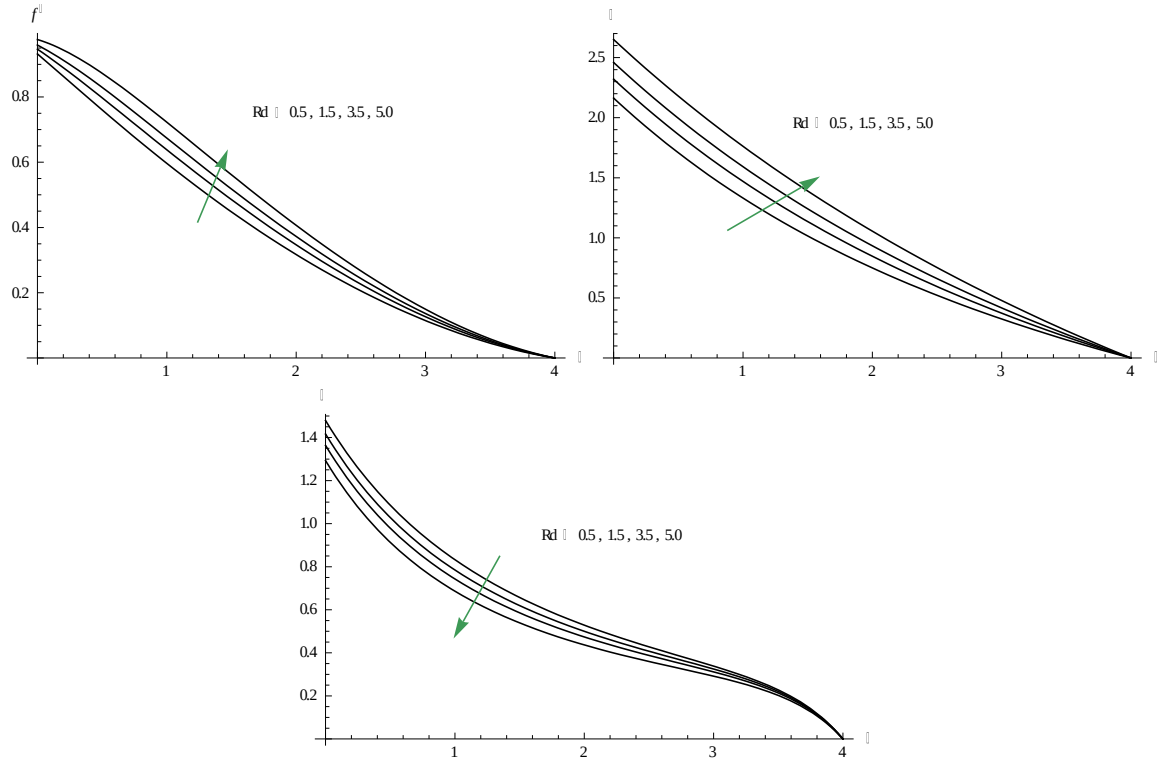

Fig.12: [a] Variation of velocity(f'), [b] Temperature(θ), [c] Nano-Concentration(ϕ) with Rd
G=2M=0.5N=0.5Ec=0.01Nb=0.3Nt=0.3
A1=0.5S=0.1fw=0.2,A=1.05,A11=0.2Le=10Pr=0.71

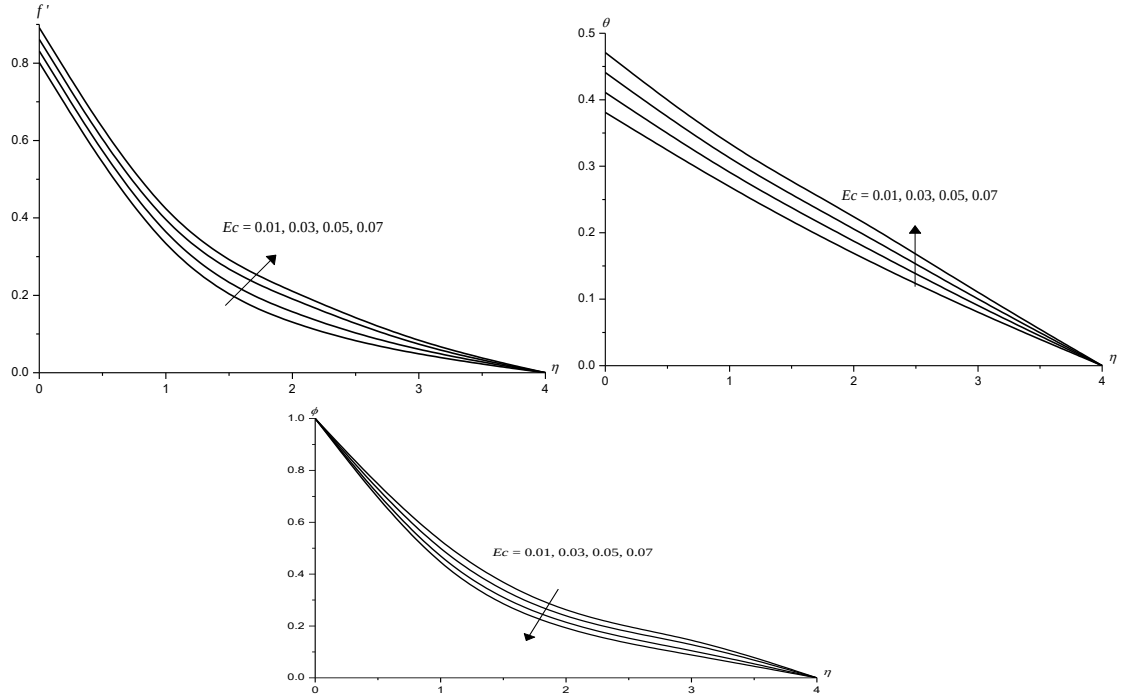

Fig.13 : [a] Variation of velocity(f'), [b] Temperature(θ), [c] Nano-Concentration(ϕ) with Ec
G=2M=0.5N=0.5Rd=0.5Nb=0.3Nt=0.3.A1=0.5,B1=0.5,
S=0.1fw=0.2,A=1.05,A11=0.2Le=10Pr=0.71

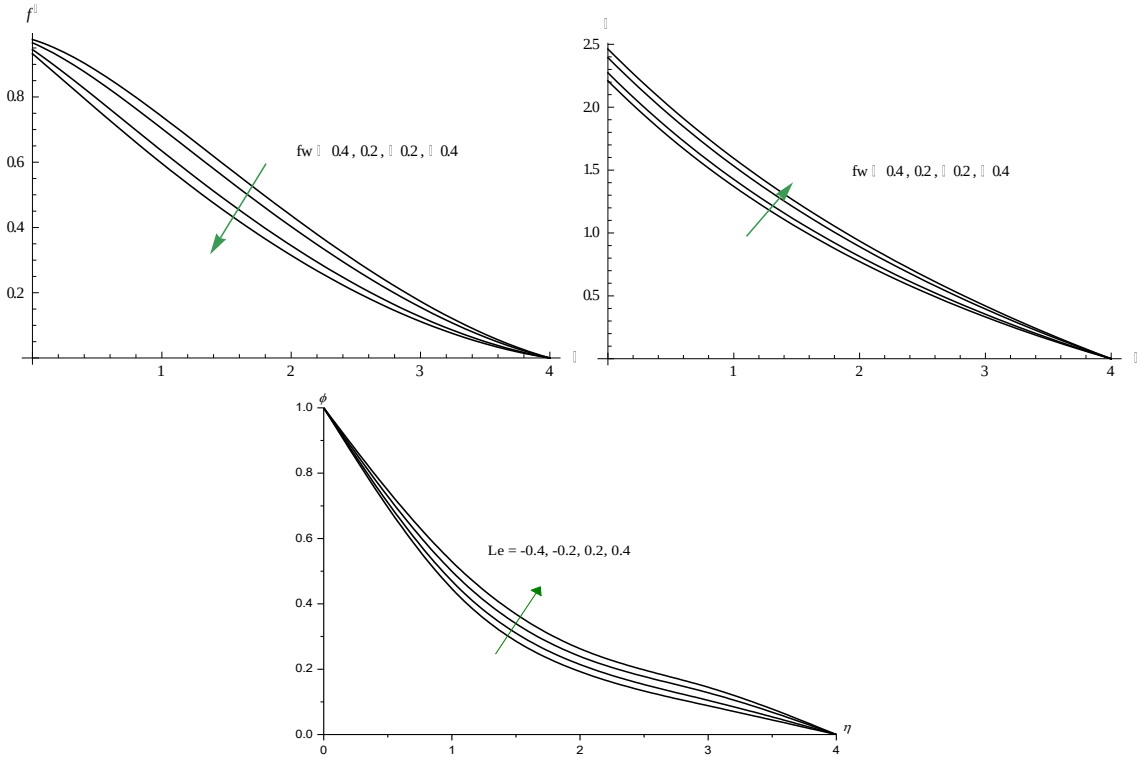

Fig.14 : [a] Variation of velocity(f'), [b] Temperature(θ), [c] Nano-Concentration(ϕ) with fw
M=0.5N=0.5Rd=0.5Ec=0.01γ=0.5Nb=0.3
Nt=0.3A1=0.5,B1=0.5,S=0.1,A=1.05,A11=0.2Le=10Pr=0.71

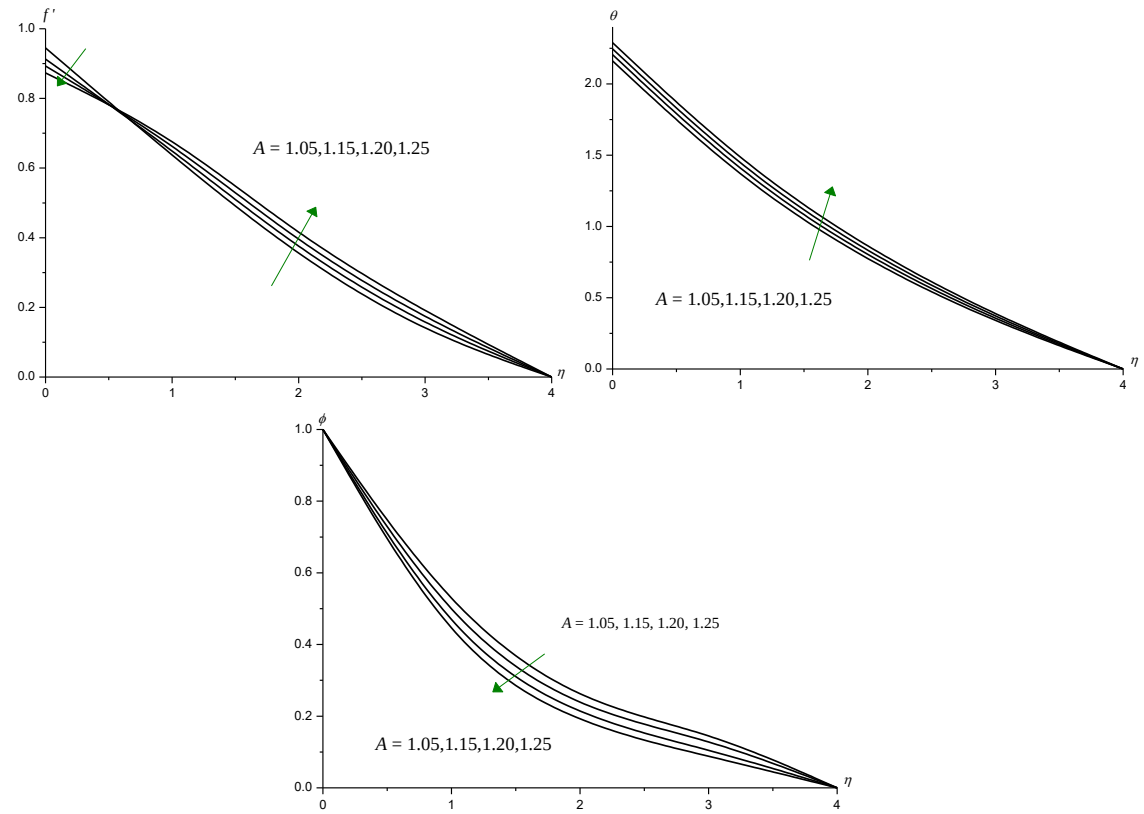

Fig.15 : [a] Variation of velocity(f'), [b] Temperature(θ), [c] Nano-Concentration(ϕ) with A
M=0.5N=0.5Rd=0.5Ec=0.01Nb=0.3Nt=0.3,A11=0.2,

A1=0.5B1=0.5S=0.1fw=0.2G=2Le=10Pr=0.71

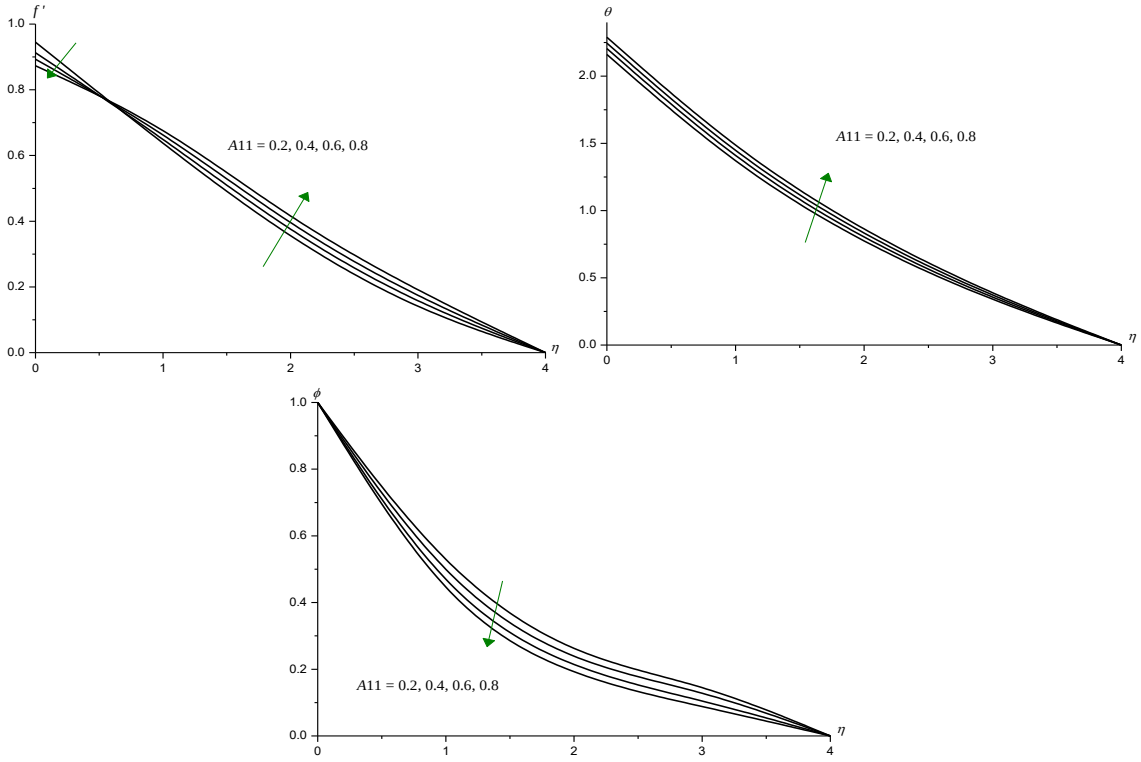

Fig. [a] Variation of velocity(f'), [b] Temperature(θ), [c] Nano-Concentration(ϕ) with A11
M=0.5N=0.5Rd=0.5Ec=0.01Nb=0.3Nt=0.3
A1=0.5B1=0.5,A=1.05,S=0.1fw=0.2G=2Le=10Pr=0.71

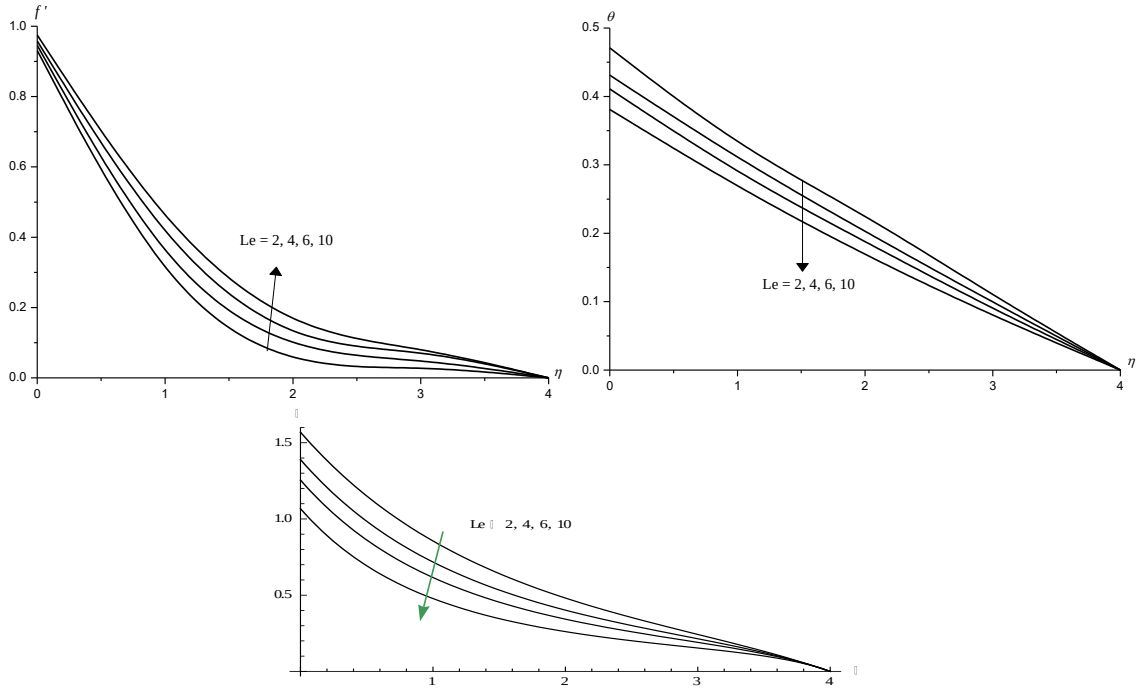

fig.17: [a] Variation of velocity(f'), [b] Temperature(θ), [c] Nano-Concentration(ϕ) with Le
M=0.5N=0.5Rd=0.5Ec=0.01Nb=0.3,A1=0.5,B1=0.5,
Nt=0.3S=0.1fw=0.2,A=1.05,A11=0.2Pr=0.71

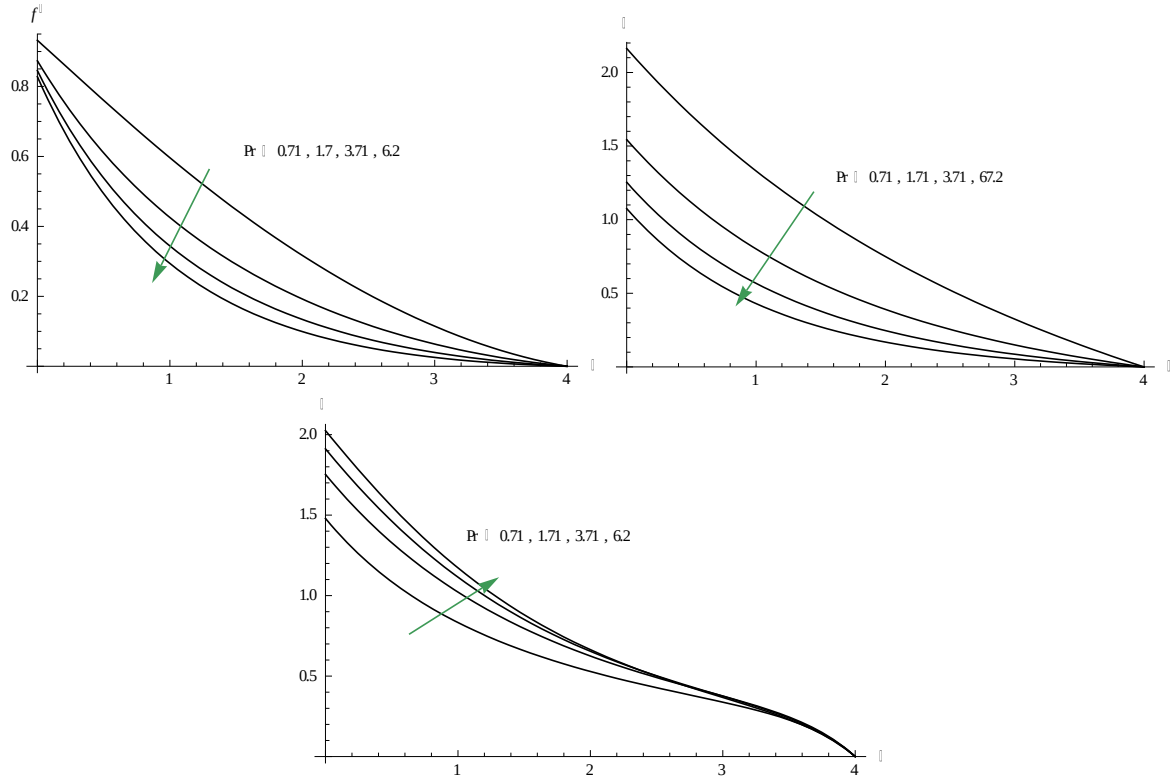

Fig.18[a] Variation of velocity(f'), [b] Temperature(θ), [c] Nano-Concentration(ϕ) with Pr
M=0.5N=0.5Rd=0.5Ec=0.01Nb=0.3Nt=0.3, A1=0.5,B1=0.5
A1=0.5B1=0.5S=0.1fw=0.2,A=1.05,A11=0.2Le=10

Table - 2
Skin Friction (τ), Nusslet number (Nu) and Sherwood Number (Sh) at η = 0

Parameter		τ(0)	Nu(0)	Sh(0)	Parameter		τ(0)	Nu(0)	Sh(0)
G	2	-0.287598	0.438313	0.69104	A1	0.5	-0.287598	0.438313	0.69104
	4	0.00563883	0.46424	0.682223		1.5	-0.245333	0.421363	0.719295
	6	0.262447	0.484916	0.669279		-0.5	-0.328013	0.456429	0.681408
	10	0.708231	0.517352	0.650639		-1.5	-0.366828	0.474776	0.664822
M	0.5	-0.287598	0.438313	0.69104	B1	0.5	-0.287598	0.438313	0.69104
	1.0	-0.351174	0.432303	0.704275		1.5	-0.181026	0.397312	0.751367
	1.5	-0.538208	0.414536	0.718703		-0.5	-0.377005	0.479728	0.661263
	2.0	-0.629398	0.405926	0.726454		-1.5	-0.451077	0.519377	0.632486
D^{-1}	0.2	-0.286972	0.438388	0.699746	S	0.1	-0.276789	0.427359	0.414141
	0.4	-0.356254	0.431963	0.704454		0.2	-0.274068	0.430484	0.492277
	0.6	-0.539495	0.415118	0.717741		0.3	-0.275815	0.432991	0.556838
	0.8	-0.740057	439718	0.733745		0.5	-0.279492	0.435291	0.617626
N	0.5	-0.287598	0.438313	0.69104	fw	0.2	-0.286972	0.438388	0.699746
	1.0	-0.369302	0.430507	0.705193		0.4	-0.351829	0.450975	0.688196
	1.5	-0.44597	0.423086	0.71054		-0.2	-0.181433	0.41654	0.722097
	2.0	-0.520861	0.415771	0.716039		-0.4	-0.129974	0.405027	0.735242
Rd	0.5	-0.287598	0.438313	0.69104	A	1.05	-0.286972	0.438388	0.699746
	1.5	0.814982	0.502352	1.09093		1.15	-0.215285	0.436274	0.702905
	3.5	-1.30758	2.24901	1.14316		1.2	-0.175535	0.435085	0.704698
	5.0	-1.31387	2.31669	1.16531		1.25	-0.148199	0.434266	0.705948
Ec	0.01	-0.287598	0.438313	0.69104	A11	0.2	-0.282023	0.436379	0.70115

	0.03	-0.286034	0.437989	0.700203		0.4	-0.211604	0.434346	0.704209
	0.05	-0.284247	0.437229	0.701072		0.6	-0.172542	0.433209	0.705945
	0.07	-0.283353	0.436853	0.701507		0.8	-0.145684	0.432423	0.707156
γ	0.5	-0.287598	0.438313	0.69104	Le	2	-0.313819	0.435584	0.44855
	1.5	-0.272706	0.43998	0.995267		4	-0.304001	0.436655	0.516048
	-0.5	-0.350377	0.430193	0.310185		6	-0.296796	0.437354	0.580307
	-1.5	-0.161237	0.45787	-0.563403		10	-0.286972	0.438388	0.699746
Nb	0.1	-0.287598	0.438313	0.69104	Pr	0.71	-0.287598	0.438313	0.691043
	0.3	-0.274193	0.439921	0.941729		1.71	-0.571567	0.597446	0.593291
	0.5	-0.271795	0.440208	1.00702		3.71	-0.710756	0.722368	0.545107
	0.7	-0.270747	0.440334	1.03848		6.2	-0.798726	0.831414	0.515198
Nt	0.1	-0.274397	0.439897	0.936572					
	0.3	-0.286972	0.438388	0.699746					
	0.5	-0.301305	0.436662	0.542968					
	0.7	-0.313656	0.435168	0.454957					

7. References

[1]. Afify, A.A. (2009). Similarity solution in MHD effects of thermal diffusion and diffusion thermos on free convective heat and mass transfer over a stretching surface considering suction or injection, Commum Nonlinear Sci Numer Simulat, Vol.14, pp.2204-2214.

[2]. Bachok, N., Ishak, A., Pop, I. (2010). Boundary-layer flow of nanofluids over a moving surface in a flowing fluid, Int J Therm Sci, Vol.49, 1663e1668.

[3]. Chamka, A.J., Issa, C. (2000). Effects of heat generation/absorption and thermophoresis on hydromagnetic flow with heat and mass transfer over a flat surface, Int Journal of Numerical Methods For Heat Fluid flow, Vol.10(4), pp.432-448.

[4]. Choi, S.U.S. (1995). Enhanced thermal conductivity of nanofluids with nano particles, development and applications of Newtonian flows. FED. vol.231/MD-vol.66, pp. 99-105.

[5]. Derjaguin, B.V., Yalamov, Y. (1965). Theory of thermophoresis of large aerosol particles, Journal of colloid science, Vol. 20, pp.555-570.

[6]. Dessie, H., and Kishan, N. (2014). Scaling group analysis on MHD free Convective Heat andMass Transfer over a stretching surface with suction/injection, Heat source/sink considering viscous dissipation and chemical reaction effects, Applications and Applied Mathematics: An International Journal, Vol.9,No.2,pp.553-572.

[7]. Ece, M.C. (2005). Free convection flow about a cone under mixed thermal boundary conditions and a magnetic field, Appl Math Model, Vol. 29, pp.1121-1134.

[8]. Ferdowsi, M., Chapal, S.M., and Afify, A. A. (2014). Boundary Layer Flow and Heat Transfer of a Nanofluid over a Permeable Unsteady Stretching Sheet with Viscous Dissipation. Journal of Engineering Thermophysics, Vol. 23, No. 3, pp. 216–228.

[9]. Ghalambaz, M., and Noghrehabadi, A. (2014). Effects of heat generation/absorption on natural convection of nanofluids over the vertical plate embedded in a porous medium using drift-flux model, Journal of computational and applied research in mechanical engineering, Vol. 3(2), pp. 113-123.

[10]. Goren, S.L. (1977). Thermophoresis of aerosol particles in laminar boundary layer on flat plate, Journal of Colloid Interface in Science, Vol. 61, pp.77-85.

[11]. Ibrahim, F.S., Elaiw, A.M., and Bakr, A.A. (2008). Influence of viscous dissipation and radiation on unsteady MHD mixed convection flow of micropolar fluids, Appl Math Inform Sci., Vol.2, pp.143-162.

[12]. Ishak, A., Nazar, R., and Pop, I. (2009). Heat Transfer over an Unsteady Stretching Permeable Surface with Prescribed Wall Temperature, Nonlin Anal Real World Appl, Vol. 10, pp.2909–2913.

[13]. Kabir, M.A., Mahbub, M.A.L. (2012). Effects of Thermophoresis on Unsteady MHD Free Convective Heat and Mass Transfer along an inclined Porous Plate with Heat Generation in Presence of Magnetic Field. Open Journal of Fluid Dynamics, Vol. 2, pp.120-129.

[14]. Manjulatha, V., Varma, S.V.K and Raju, V.C.C. (2014). Effects of Radiation Absorption and Mass Transfer on the Free Convective Flow Passed a Vertical Flat Plate through a Porous Medium in an Aligned Magnetic Field, Applications and Applied mathematics: Aninternational jouranal,Vol.9,No.1, pp.75-93.

[15]. Mohan Krishna, P., Sugunamma, V., and Sandeep, N. (2014). Radiation and magneticfield effects on unsteady natural convection flow of a nanofluid past an infinite vertical plate with heat source, Chemical and Process Engineering Research, Vol 25, pp39-52.

[16]. Noor, N.F.M., Abbansbandy, S., Hasim, I. (2013). Heat and mass transfer of thermophoretic MHD flow over an inclined radiative isothermal permeable surface in presence of heat source/sink, Int J Heat and Mass Transfer, Spl. Issue 2013, pp.1-23.

[17]. Philip, I., Shima, J.P.D., and Raj, B. (2008). Nanofluid with tunable thermal properties, Appl phys Lett, 92.043108.

[18]. Prasad, K.V., Pal, D., Umesh, V., and Rao, N.S.P. (2010). The effect of variable viscosity on MHD viscoelastic fluid flow and heat transfer over a stretching sheet, Commun Nonlinear Sci Numer Simul, Vol.15, pp.331-344.

[19]. Rushi Kumar, B. (2013). MHD boundary layer flow on heat and mass transfer over a stretching sheet with slip effect, Journal of Naval Architecture and Marine Engineering, Vol 10 (2), pp.16-26.

[20]. Sandeep, N., Reddy, A.V.B., Sugunamma, V. (2012). Effect of radiation and chemical reaction on transient MHD free convective flow over a vertical plate through porous media, Chemical and process engineering research, Vol. 2, pp.1-9.

[21]. Sandeep, N., Sugunamma, V., and Mohankrishna, P. (2013). Effects of radiation on an unsteady natural convective flow of a EG-Nimonic80a nanofluid past an infinite vertical plate, Advances in Physics Theories and Applications, Vol. 23, pp.36-43.

[22]. Sandeep,N, Sulochana,C. Raju, C.S.K. Jayachandra Babu, M. Sugunamma, V: Unsteady boundary layer flow of thermophoretic MHD nanofluid past a stretching sheet with space and time dependent internal heat source/sink *International Journal of Applications and Applied Mathematics* (IJAAM), Vol. 10, Issue 1, pp. 312-327, (June 2015), ISSN: 1932-9466, http://pvamu.edu/aam

[23]. Seddeek M.A., Darwish, A.A., Abdelmeguid, M.S. (2007). Effects of Chemical Reaction and Variable Viscosity on Hydro magnetic Mixed Convection Heat and Mass Transfer for Hiemenz Flow Through Porous Media with Radiation, Commun Nonlinear Sci Numer Simulat, Vol.12, pp.195-213.

[24]. Seth, G. S., Mahto, N., Ansari, Md. S., and Nandkeolyar, R. (2010). Combined free and forced convection flow in a rotating channel with arbitrary conducting walls, Int J Eng Sci Tech, Vol. 2(5), pp.184–197.

[25]. Tsai, R. (1999). A simple approach for evaluating the effect of wall suction and thermophoresis on aerosol particle deposition from a laminar flow over a flat plate, International Communication Heat & Mass Transfer, Vol.26, pp.249–257.

[26]. Uddin, M.J., Beg, O.A., and Ismail, A.I. Md. (2014). Mathematical modeling of Radiative Hydro magnetic Thermosolutal Nanofluid convection slip flow in saturated porous media, Math Probs in Eng, Vol.2014, pp1-11.

[27]. Yasin, M.H.M., Arifin, N.M., Nazar, R., Ismail, F., and Pop, I. (2013). Mixed convection boundary Layer flow embedded in thermally stratified porous medium saturated by a nanofluid, Advances in Mechanical engineering, http://dx.doi.org/10.1155/2013/121943.